The Structure of Nucleotidylated Histidine-166 of Galactose-1-phosphate Uridylyltransferase Provides Insight into Phosphoryl Group Transfer[†,‡]

Joseph E. Wedekind,[§] Perry A. Frey,* and Ivan Rayment*

Institute for Enzyme Research, Graduate School, and Department of Biochemistry, College of Agricultural and Life Sciences, University of Wisconsin−Madison, Madison, Wisconsin 53705

Received May 29, 1996; Revised Manuscript Received July 1, 1996[⊗]

ABSTRACT: Galactose-1-phosphate uridylyltransferase catalyzes the reaction of UDP-glucose with galactose 1-phosphate to form UDP-galactose and glucose 1-phosphate during normal cellular metabolism. The reaction proceeds through a double displacement mechanism characterized by the formation of a stable nucleotidylated histidine intermediate. This paper describes the preparation of the uridylyl-enzyme complex on the crystalline enzyme from *Escherichia coli* and its subsequent structure determination by X-ray crystallography. The refined structure has an *R*-factor of 19.6% (data between 65 and 1.86 Å resolution) and reveals modest conformational changes at the active site compared to the inactive UMP/UDP-enzyme complex reported previously [Wedekind, J. E., Frey, P. A., & Rayment, I. (1995) *Biochemistry 34*, 11049−11061]. In particular, positions of the respective UMP α-phosphoryl groups differ by ∼4 Å. Well-defined electron density for the nucleotidylated imidazole supports the existence of a covalent bond between Nϵ2 of the nucleophile and the α-phosphorus of UMP. A hydrogen bond that is conserved in both complexes between His 166 Nδ1 and the carbonyl O of His 164 serves to properly orient the nucleophile and electrostatically stabilize the positively charged imidazolium that results from nucleotidylation. Hydrogen bonds from side-chain Gln 168 to the nonbridging phosphoryl oxygens of the nucleotidyl intermediate appear crucial for the formation and reaction of the uridylyl-enzyme complex as well. The significance of the latter interaction is underscored by the fact that the predominant cause of the metabolic disease galactosemia is the mutation of the corresponding Gln (Gln 188 in humans) to Arg. A comparison to other phosphohistidyl enzymes is described, as well as a revised model for the mechanism of the uridylyltransferase.

Nucleotidyltransferases catalyze the covalent modification of a variety of biological molecules. These reactions are crucial for the synthesis of coenzymes, cyclic nucleotides, polynucleotides, and nucleotide sugars. These reactions involve substitutions at the α-phosphorus of a nucleotidyl donor substrate and result in displacement of a phosphoryl ester or pyrophosphate. Substrates for such reactions may include nucleoside di- or triphosphates, as well as nucleotide sugars, such as UDP-Glc.[1]

Galactose-1-phosphate uridylyltransferase (hexose-1-phosphate uridylyltransferase EC 2.7.7.12) catalyzes the exchange of the UMP moiety between the hexose 1-phosphates of Glc and Gal and their corresponding UDP-sugars as depicted in eq 1. The enzyme is distinct among

$$\text{Gal-1-P} + \text{UDP-glucose} \rightleftarrows \text{UDP-galactose} + \text{Glc-1-P} \quad (1)$$

nucleotidyl transferases that use phosphates as acceptor groups in that it is the only one that does not utilize nucleoside di- or triphosphates as the nucleotidyl donor substrate. The reaction is part of the Leloir pathway of galactose metabolism required for the normal equilibration of UDP-hexoses among most organisms. Deficiencies in uridylyltransferase activity culminate in the metabolic disease galactosemia, which occurs as an autosomal recessive trait (Kalckar, 1960; Levy & Hammersen, 1978).

Kinetic and chemical properties of the uridylyltransferase reaction have been characterized most extensively for the enzyme from *Escherichia coli*. The reaction exhibits ping-pong kinetics (Wong & Frey, 1974a,b) and proceeds with retention of configuration about the α-phosphorus *via* two inversion steps (Sheu et al., 1979; Arabshahi et al., 1986). Kinetic and chemical properties for this enzyme have been confirmed in part for the yeast and human enzymes as well (Wu et al., 1974; Markus et al., 1977; Segawa & Fukasawa, 1979). The double displacement reaction scheme is depicted in eqs 2 and 3. In the course of the reaction, a nucleophilic

$$\text{UDP-Glc} + \text{E-His} \rightleftarrows \text{Glc-1-P} + \text{E-His-UMP} \quad (2)$$

[†] Supported by Grant AR35186 from the National Institute of Arthritis, Musculoskeletal and Skin Diseases (I.R.), by Grant GM30480 from the National Institute of General Medical Sciences (P.A.F.), and by an NRSA fellowship (J.E.W.) from NIH Training Grant GM08293.

[‡] The X-ray coordinates have been deposited in the Brookhaven Protein Data Bank (file name 1HXQ).

* Address correspondence to these authors at the Institute for Enzyme Research, University of Wisconsin, 1710 University Ave., Madison, WI 53705. Phone: 608-262-0437 (I.R.). Phone: 608-262-0055 (P.A.F.). Fax: 608-265-2904.

[§] Present address: Department of Structural Biology, Fairchild Center, Stanford University School of Medicine, Stanford, CA 94305-5400.

[⊗] Abstract published in *Advance ACS Abstracts,* August 15, 1996.

[1] Abbreviations: Gal, galactose; Glc, glucose; UDP-Glc, uridine 5′-diphosphate glucose; UDP-Gal, uridine 5′-diphosphate galactose; UMP, uridine 5′-monophosphate; UDP, uridine 5′-diphosphate; Glc-1-P, glucose 1-phosphate; Gal-1-P, galactose 1-phosphate; hexose-1-P, hexose 1-phosphate; phenyl-UDP, P^1-5′-uridine P^2-phenyl diphosphate; NDP kinase, nucleoside diphosphate kinase; HPr, histidine-containing phosphocarrier protein; PEG, poly(ethylene glycol); MES, 2-(*N*-morphilino)ethanesulfonic acid; HEPES, *N*-(2-hydroxyethyl)piperazine-*N*′-2-ethanesulfonic acid; rms, root mean square; PDB, Brookhaven Protein Data Bank; UMPIm, uridine 5′-phosphoimidazolate; SCS, succinyl-CoA synthetase.

S0006-2960(96)01267-6 CCC: $12.00

$$\text{Gal-1-P} + \text{E-His-UMP} \rightleftarrows \text{UDP-Gal} + \text{E-His} \quad (3)$$

histidine is uridylylated, forming a stable covalent uridylyl-enzyme adduct (Wong & Frey, 1974a; Wong et al., 1977). The modification was reported to occur at position Nδ1 of the imidazole ring (Yang & Frey, 1979). This histidine has been identified as residue 166 in the enzyme from *E. coli* (Field et al., 1989; Kim et al., 1990). Although the pH optimum for the uridylyltransferase reaction occurs between pH 8.4 and pH 8.9 for the *E. coli*, yeast, and calf liver enzymes (Maxwell et al., 1962; Segawa & Fukasawa, 1979), the uridylyltranferase from yeast retains approximately 53% of maximal activity at pH 7.1 (Fukasawa et al., 1982).

The structures of several proteins that contain phosphohistidyl modifications have been reported recently. Such structures represent either genuine enzymatic reaction intermediates or the phosphorylated state of specific phospho-carrier proteins. Wolodko et al. (1994) described the first such intermediate for succinyl-CoA synthetase. Similarly, the phosphohistidyl intermediate of NDP kinase has been characterized by both X-ray crystallographic and NMR techniques (Lecroisey et al., 1995; Moréra et al., 1995). Phosphorylated histidines have been examined by NMR for protein III^{Glc} and HPr of the phosphoenolpyruvate−glycose phosphotransferase system as well (Pelton et al., 1992; van Nuland et al., 1995). However, there has been (to our knowledge) no structural report of a phosphoramidate nucleotidyl-enzyme intermediate.

Here we present the crystal structure of the uridylyl-enzyme intermediate of galactose-1-phosphate uridylyltransferase at a resolution of 1.86 Å. This study was undertaken to provide a structural framework for understanding the existing structural and mechanistic studies of this enzyme. In particular, we wished to identify the groups involved in the formation and stabilization of the covalent intermediate, as well as the localized structural changes involved in intermediate formation, since a significant conformational change in the position of the UMP α-phosphorus was anticipated (Wedekind et al., 1995). It was observed in the present study that the phosphoramidate forms between the α-phosphorus of UMP and Nϵ2 of His 166 which requires reevaluation of the earlier chemical studies that reported modification at position Nδ1 (Yang & Frey, 1979). The structure also provides a molecular explanation for the predominant form of human galactosemia that arises from mutation of a residue that forms a significant number of hydrogen bond interactions to the nucleotidylated histidine. In addition, a comparison to other phosphohistidyl-containing enzymes illustrates common features that contribute to phosphoramidate stability. The structure forms the basis for a revised model for the reaction and presents new questions regarding the binding site for the hexose 1-phosphate.

EXPERIMENTAL PROCEDURES

Protein Purification and Crystallization. Galactose-1-phosphate uridylyltransferase was purified and crystallized as described previously (Wedekind et al., 1994). Crystals were grown by vapor diffusion from ~14% (w/v) PEG 10000, 0.40 M Li_2SO_4, 0.25 M NaCl, and 0.10 M sodium succinate at pH 6. Phenyl-UDP (0.004 M) was substituted with 0.005 M sodium UMP (Sigma Chemical Co., St. Louis, MO). β-Mercaptoethanol (BME) (1 mM) was present during the subsequent manipulation of the crystals, rather than the 10 mM incorporated in the original crystallization.

Formation of the Uridylyl-Enzyme and Cryoprotection. Single crystals approximately 0.2 × 0.3 × 1.0 mm were transferred into 0.3 mL volumes of a synthetic mother liquor devoid of Li_2SO_4. Sulfate was removed from the crystals in order to avoid competition for the UDP-hexose binding site on the enzyme. The initial synthetic mother liquor was composed of 18% (w/v) PEG 10000, 0.80 M NaCl, and 0.10 M sodium succinate at pH 6.0. Crystals were incubated in this solution for 45 min at 4 °C and subsequently transferred to a fresh "reaction" solution containing 0.005 M NaUDP-Glc (approximately 25-fold greater than K_m; Wong & Frey, 1974a). An increase in the concentration of PEG in the absence of substrate was necessary to prevent severe cracking of the crystals in the ensuing reaction steps. Even so, crystals developed minor cracks upon initial introduction of substrate, although these promptly reannealed.

At 30 min intervals, crystals were transferred to fresh reaction solutions buffered at successively higher pH values. Under such conditions the enzyme is more active whereas the rate of acid-catalyzed hydrolysis of the intermediate is reduced. First, the pH was increased to 6.4 by substitution of sodium succinate with NaMES; the pH was raised subsequently to 7.1 by substitution with NaHEPES. Attempts to increase the crystal pH beyond 7.9 were unsuccessful as judged by the quality of the resulting X-ray diffraction data and electron density maps. Prolonged exposure to elevated pH ≥7 causes crystals to dissolve. Prior to the introduction of cryoprotectant, crystals were transferred to a reaction solution of 22% (w/v) PEG 10000, 0.95 M NaCl, and 0.005 M UDP-glucose buffered by 0.10 M HEPES; crystals were incubated for 2 h. At 6 min intervals, crystals were transferred to the latter synthetic mother liquor containing successively higher amounts of ethylene glycol (5.3%, 10.7%, and 16%). Crystals were captured on thin nylon loops (approximately 0.8 mm in diameter) and flash cooled in a stream of nitrogen gas to approximately −160 °C (Teng, 1990; Rodgers, 1994).

X-ray Data Collection and Processing. X-ray intensities were recorded on a Siemens Hi-STAR dual detector system at crystal-to-detector distances of 15.0 and 24.2 cm using the 1024 and 512 pixel formats, respectively. X-rays were generated by a Rigaku RU200 rotating anode operated at 50 kV by 50 mA equipped with Supper double-focusing mirrors. Crystals of the uridylyltransferase belong to space group $P2_12_12$ (Wedekind et al., 1994). Upon cooling, the unit cell volume decreased by approximately 4%. The resulting lattice parameters were $a = 57.2$ Å, $b = 215.4$ Å, and $c = 68.9$ Å. An initial low-resolution data set was collected to 2.4 Å resolution in order to verify uridylylation, followed by subsequent data collection from a second crystal to 1.86 Å resolution. The data frames from the two crystals were processed with the SAINT data reduction software and scaled with the program XSCALIBRE (G. Wesenberg and I. Rayment, unpublished results). The R_{merge} for 206 202 observations between 65 and 1.86 Å resolution was 6.4%. This reduced to 70 581 independent reflections, providing a

Table 1: Intensity Statistics for the Native Data X-ray Data Set

	shell (Å)						
	total	65−3.38	−2.68	−2.34	−2.13	−1.98	−1.86
exptl observations	206202	64170	47934	32187	22351	20475	19085
singlet measurements	15045	389	252	1806	3655	4289	4654
independent reflections	70581	12490	12136	12004	11667	11300	10989
completeness (%)	97	99	99	99	99	96	90
intensity (av)	4268	10000	3005	1338	1017	837	599
σ (av)	141	181	144	106	105	118	122
R-factor (%)[a]	6.25	5.6	7.0	8.7	9.4	12.1	16.5

[a] $R\text{-factor} = \sum|I_j - \bar{I}|/\sum|I_j| \times 100$.

data set that is 90% complete in the highest resolution shell. Data collection statistics are shown in Table 1.

Structure Determination and Refinement. The starting model for refinement was based upon the atomic coordinates of the UMP/UDP enzyme structure reported at 1.8 Å resolution [Wedekind et al., 1995; see PDB entry 1HXP (Bernstein et al., 1977)]. Solvent molecules and the uridine nucleotides were removed from the dimeric model prior to the initiation of refinement. In addition, the following residues were excluded: His 27 through Ala 36 (subunit I) and His 27 through Ala 29 (subunit II). The initial *R*-factor calculated for all data between 65 and 2.4 Å resolution was 36.7%. The model was refined against data between 65 and 2.0 Å resolution with the program TNT (Tronrud et al., 1987) to an *R*-factor of 25.7%. Subsequent manual rebuilding and adjustments to the model were made with the program FRODO (Jones, 1985). Electron density maps with coefficients ($2F_o - F_c$) and ($F_o - F_c$) were displayed on an Evans and Sutherland PS390 interactive graphics system. Solvent atoms were initially assigned by use of the programs PEAKMAX, WATPEAK, and DISTANG in the CCP4 program suite (CCP4, 1994). Atoms were assigned as solvent, provided they appeared ≤4.0 Å from a suitable hydrogen bond partner and provided a signal ≥2.0σ in ($F_o - F_c$) electron density maps. After further refinement with all of the data to 1.86 Å resolution the uridylylated histidine was modeled. Target geometries for the intermediate model were derived from the structures of 1-(carboxymethyl)-2-imino-3-phosphonoimidazolidine (Phillips et al., 1979) and Na_2UMP (Seshadri et al., 1980).

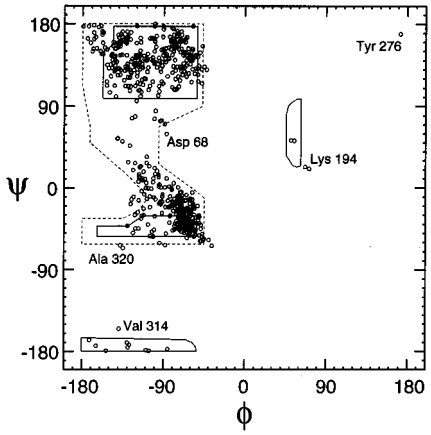

FIGURE 1: Ramachandran plot of the main-chain non-glycinyl dihedral angles for the dimeric enzyme model. Fully allowed ϕ, ψ values are shown by solid enclosures. Partially allowed regions are enclosed by broken lines. Outliers such as Asp 68 (subunit I), Ala 320 (subunits I and II), and Lys 194 can be attributed to hydrogen bonding [as seen in the previous structure by Wedekind et al. (1995)]. Tyr 276 (subunit I) and Val 314 (subunit II) were not outliers in the previous structure. The hydroxyl group of Tyr 276 forms hydrogen bonds to Oϵ of Glu 152 (strand β7) and an ordered solvent molecule in both subunits. Its dihedral angles reside in the unallowed ($\phi = 171°$, $\psi = 169°$) and partially allowed ($\phi = -179°$, $\psi = 177°$) regions. As a result of UMP binding (strands β3, β6, β7, and β8), changes in the local solvent distribution may explain the unfavorable dihedral angle changes compared to the previous structure. Val 314 is an outlier in subunit II, due to the absence of an intermolecular hydrogen bond contact observed in subunit I. In the latter subunit, the amide of Gly 315 interacts with Oδ of Asn 153 to provide stability to this surface loop. This region has been made asymmetric by crystal contacts.

RESULTS AND DISCUSSION

Refined Model. The present dimeric model is composed of residues 2 through 35 and 45 through 348 of subunit I and residues 2 through 30 and 44 through 346 of subunit II. The model includes 730 solvent molecules that all have *B*-factors <99 Å^2. Uridylylated His 166 has been modeled with full occupancy in both subunits. The present crystallographic *R*-factor is 19.6% for all measured data between 65 and 1.86 Å resolution. The rms deviation from the target geometry is 0.013 Å for bond lengths, 2.1° for bond angles, 16.2° for torsional angles, 0.003 Å for trigonal planes, and 0.005 Å for groups of atoms expected to be coplanar. A Ramachandran plot of all main-chain non-glycinyl dihedral angles is provided in Figure 1.

Polypeptide Fold. Galactose-1-phosphate uridylyltransferase from *E. coli* is a dimer of chemically identical subunits. Each subunit is composed of 348 amino acids and includes two tightly associated metal ions, identified as iron and zinc (Ruzicka et al., 1995). The dimeric structure of the UMP/UDP uridylyltransferase complex from *E. coli* has been described previously to 1.8 Å resolution (Wedekind et al., 1995). Each subunit folds as a single $\beta_6\alpha\beta_2\alpha_2\beta_3\alpha\beta_2\alpha\beta\alpha$ domain. Due to the modification of Cys 160 by a BME in the UMP/UDP complex, the original structure is that of an inactive enzyme. Inhibition by BME blocks access to the active site nucleophile, resulting in nonproductive binding and partial disorder of the nucleotide at its α- and β-phosphates. There is no modification of Cys 160 in the present structure. Thus, even though the uridylyl intermediate structure closely resembles the starting model, the model reported here represents a genuine intermediate of the nucleotidyltransferase reaction in which the α-phosphorus of UMP forms a covalent bond to His 166. The average error in the model is estimated to be between 0.15 and 0.175 Å, based upon a Luzzati analysis (Luzzati, 1952) shown in Figure 2. A representative section of electron density is shown in Figure 3.

The rms deviation for the superposition of all atoms from the respective dyad-related subunits of the refined uridylyl-

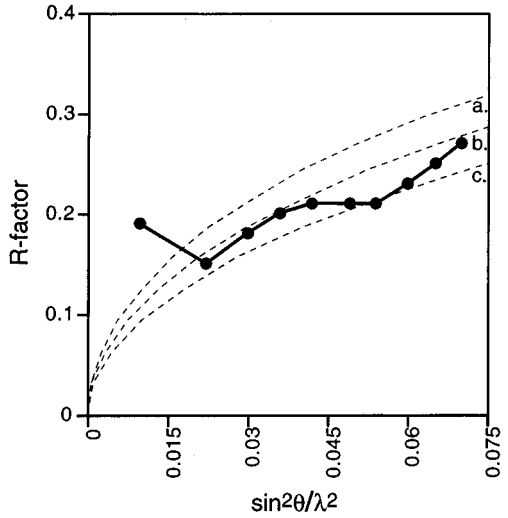

FIGURE 2: Plot of the crystallographic *R*-factor for the uridylyl-enzyme intermediate as a function of resolution (expressed as $\sin^2\theta/\lambda^2$). Theoretical variations of the *R*-factor, Δr, for coordinate errors 0.15, 0.175, and 0.20 Å are indicated by the broken curves labeled a, b, and c, respectively.

enzyme model is 0.27 Å. Superpositions were calculated with the program LSQKAB implemented in the CCP4 program package (Kabsch, 1976; CCP4, 1994). The rms deviation between the UMP/UDP complex and the uridylyl intermediate for all equivalent pairs of protein atoms is 0.74 Å, excluding residues 30 through 35 of subunit I. The latter region is located on the protein surface and appears to adopt a conformation different from that reported previously (Wedekind et al., 1995). Changes are due possibly to the introduction of cryoprotectant or elevation of the crystal pH from 5.9 to 7.1, which was necessary to prepare the uridylyl intermediate within the crystal lattice.

Temperature Factors. The average temperature factor for all atoms of the model is 21.6 Å^2. The average temperature factors for all atoms of subunits I and II are 19.0 and 19.9 Å^2, respectively. The average solvent temperature factor is 36.6 Å^2. Plots of the subunit I mean main-chain temperature factors for the uridylyl-enzyme (−160 °C) and UMP/UDP enzyme complexes (4 °C) (Wedekind et al., 1995) are shown in Figure 4, where the mean temperature factor for subunit I in the UMP/UDP complex was 23.3 Å^2. This plot indicates that corresponding temperature factors follow similar trends, although the solvent-exposed loop containing Cys 160 (residues 156 through 163) has significantly lower *B*-factors in the uridylyl-enzyme complex (Figure 4). This result is best explained by the direct interaction of the Cys 160 thiol with O1 of the UMP phosphoryl group. An explanation for the reduction of temperature factors in the C-terminus of the protein is less obvious.

Uridylylated His 166. Figure 5 shows representative ($F_o - F_c$) electron density calculated from the final refined phases in which the uridylylated histidine was excluded from the model beginning at the Cα of residue 166. It is apparent that Nε2 is uridylylated rather than position Nδ1 that was deduced from earlier chemical studies (Wong et al., 1977; Yang & Frey, 1979). This is a well-defined part of the electron density where the average *B*-factor for the UMP moiety is 19.8 Å, which is comparable to the average main-chain *B*-factors reported for each subunit. The imidazole orientation is in agreement with the previous model of the enzyme reported to 1.8 Å resolution (Wedekind et al., 1995). Small rotations about the χ1 side-chain dihedral angle have unfavorable steric consequences in the presence and absence of covalently bound UMP. Similarly, it is impossible to rotate the imidazole ring by a 180° rotation about χ2 since this places Cδ2 unfavorably close to the His 164 carbonyl oxygen. Such a rotation also precludes access to the α-phosphorus by either imidazolium nitrogen. In both the present and previous uridylyltransferase structures, Nδ1 is likely to be protonated, since the non-hydrogen distance between Nδ1 and the carbonyl oxygen of His 164 is approximately 2.5 Å. This observation has important implications for both the nucleophile orientation and the electrostatic state of the imidazolium leaving group during the course of the double-displacement reaction.

Previous studies of the uridylyl-enzyme intermediate concluded that the phosphoramidate linkage occurs between Nδ1 of the imidazole and the α-phosphorus of UMP (Wong et al., 1977; Yang & Frey, 1979). This report was based on a procedure designed to isolate the nucleotidylated amino acid, followed by chemical degradation of the furanose and subsequent chromatographic characterization of the remaining phosphohistidyl adduct (Yang & Frey, 1979). Since the peptide bonds of the uridylyl-enzyme were hydrolyzed by

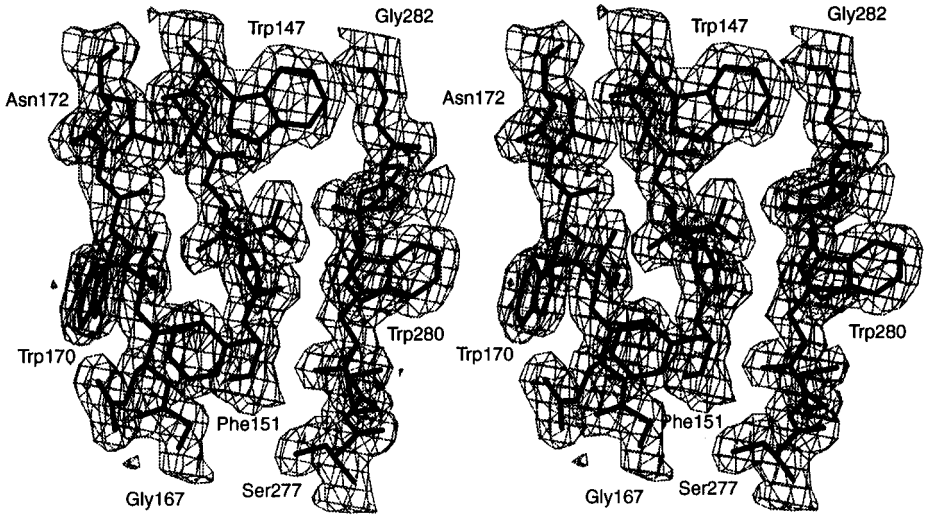

FIGURE 3: Stereoview of representative ($2F_o - F_c$) electron density for the β-sheet that underlies the active site of the Gal-1-P uridylyltransferase uridylyl-enzyme complex calculated with the final refined phases. The electron density is contoured at 1σ.

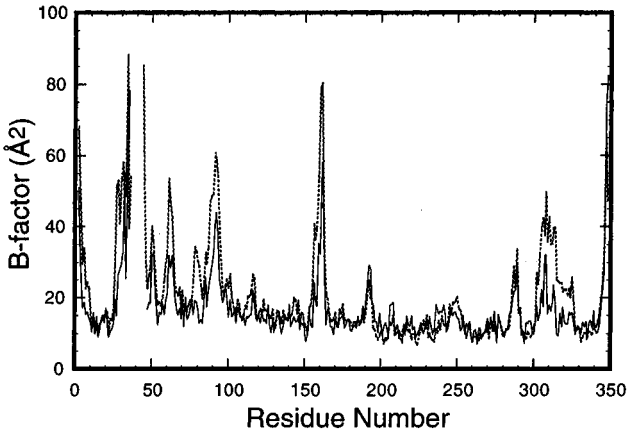

FIGURE 4: Plot of the mean *main-chain* atomic temperature factor *versus* amino acid residue for subunit I of the uridylyl-enzyme complex (solid dark lines) and the UMP/UDP enzyme complex (broken lines). Temperature factors are shown for residues 2 through 35 and residues 45 through 348 of the uridylyl-enzyme intermediate and residues 2 through 35 and residues 44 through 348 of the UMP/UDP enzyme complex (PDB entry 1HXP). X-ray data were collected at −160° and 4 °C, respectively.

use of 3 M sodium hydroxide at 110 °C, it appears likely that the phosphohistidine underwent extensive transphosphorylation to produce the favored Nδ1-phosphohistidine product. Rapid conversion of UMP-4-MeIm into a mixture of UMP-4-MeIm and UMP-5-MeIm occurs under mild conditions at ambient temperatures where the UMP-5-MeIm product is thermodynamically favored 3 to 1 over UMP-4-MeIm (Ruzicka & Frey, 1993). This may account for the predominant amount of Nδ1-phosphohistidine over Nϵ2-phosphohistidine reported (Yang & Frey, 1979). It should be noted that uridylylation of Nϵ2 is fully consistent with the stereochemical course of the reaction (Sheu et al., 1979; Arabshahi et al., 1986), whose determination was independent of the assignment of a particular nitrogen as the participant in phosphoramidate formation.

Nucleotide Binding. A portion of the active site obtained from a superposition of the UMP/UDP structure upon that of the uridylyl-enzyme complex is shown in Figure 6a. The superposition was prepared by a least-squares fit of the corresponding subunit Cα atoms, excluding residues 159 through 164. The resulting rms deviation was 0.34 Å for the protein atoms and a range of 0.63−7.0 Å for atoms of the nucleotide. It is apparent from Figure 6a that there are only subtle changes in the position of the uracil ring, whereas the ribose and phosphate positions have been altered significantly. Figure 6b shows a schematic representation of the interactions between the enzyme and nucleotide observed in the UMP/UDP enzyme complex compared to those of the uridylyl-enzyme structure. Interestingly, the hydrogen bond interactions to the respective nucleosides are maintained well despite the 4 Å migration of the α-phosphorus toward the nucleophile. The adjustments between the nucleotide and enzyme that contribute to the preservation of specific interactions between the uridylyltransferase structures suggest these changes might occur when proceeding from a precatalytic to a reaction intermediate state.

The Cys 160 Loop and the Phosphoryl Group. The nonbridging oxygens of the α-phosphoryl group, O1 and O2, make close contacts to the side chains of Cys 160 and Gln 168, as well as two ordered solvent molecules in the uridylyl-enzyme complex (Figure 6b). These interactions were not present in the previous inactive structure (Wedekind et al., 1995) due to the obstruction of the active site by BME-modified Cys 160 (Figure 6a). In the present structure, Cys 160 is unmodified, and O1 and O2 are deprotonated since uridylylation of His 166 occurred at pH 7. Consequently, the loop containing Cys 160 (residues 159−165) has moved 0.45−0.65 Å as measured by changes in the positions of its α-carbons (Sγ of Cys 160 has moved ~2.4 Å) relative to its location in the UMP/UDP enzyme complex. This suggests that a significant, though modest, conformational adjustment may be necessary to properly bind the nucleotide. Loop movement originates about the ϕ dihedral angle of Gly 159 (Figure 6a), which is a strictly conserved residue (Table 2). Flexibility of the backbone appears to terminate at His 164 due to coordination of the latter residue to a "structural" Zn^{2+} ion (Figure 6a). This ligation assures that the nucleophile His 166 will be positioned productively for catalysis.

A significant aspect of the Cys 160 loop movement appears to be the formation of hydrogen bonds to O1, O2, and O5′ of the nucleotide phosphoryl group. The thiol of

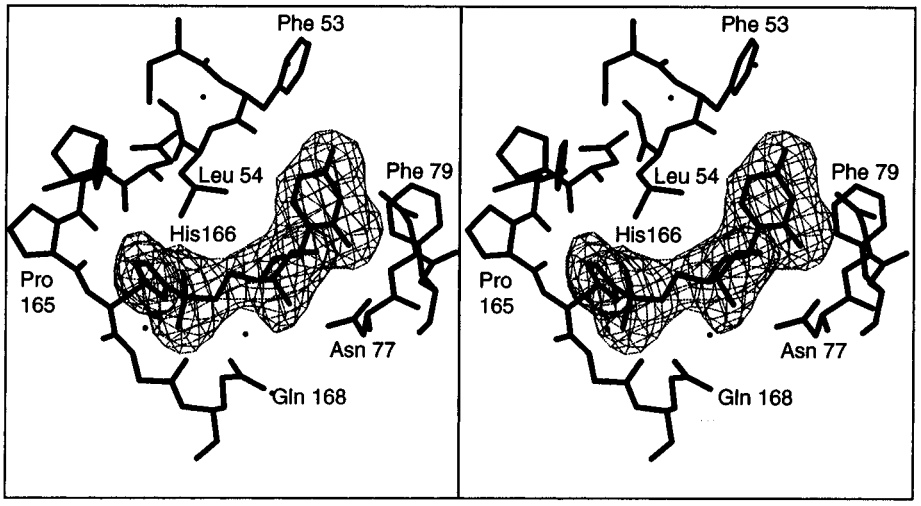

FIGURE 5: Stereoview of representative ($F_o - F_c$) electron density for uridylylated His 166 of subunit I, calculated with the final refined phases. The UMP moiety and the imidazolium side chain were removed from the model (beginning at Cα) prior to refinement. The electron density map, contoured at 3σ, indicates the phosphoramidate bond is in the imidazolium plane. Additional residues of the enzyme are shown to indicate important elements of nucleotide recognition; this includes the side chains of Asn 77, Asp 78, Phe 79, and Gln 168.

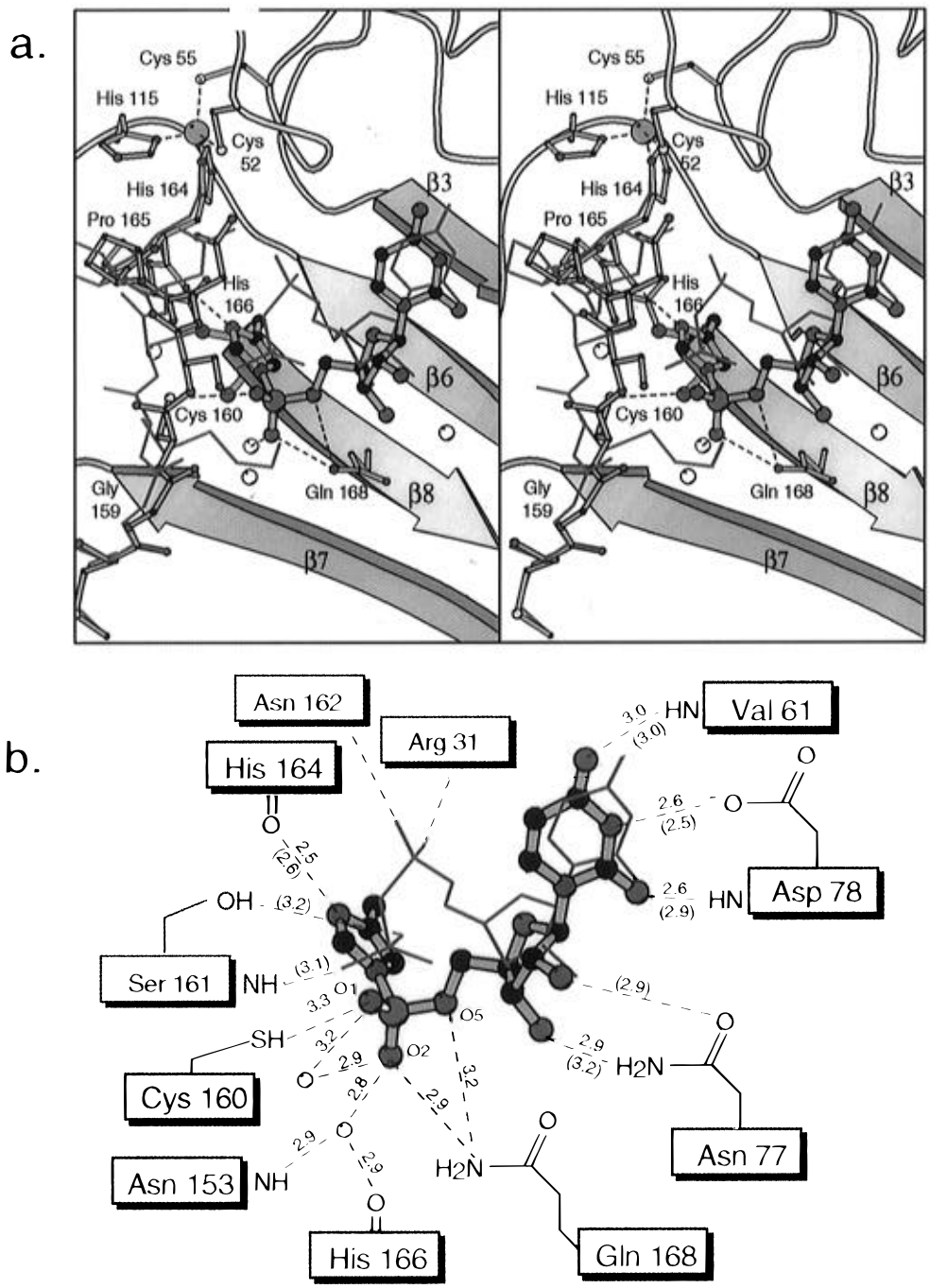

FIGURE 6: The nucleotide binding site of the uridylyl-enzyme complex (subunit II). The orientation is similar to that in Figure 5. (a) Stereo diagram illustrating the active site topology. Antiparallel strands β3, β6, β7, and β8 contribute to the formation of the nucleotide binding cleft. Red lines indicate the superimposed coordinates of the Cys 160 loop from the UMP/UDP complex (PDB entry 1HXP) upon the uridylyl-enzyme complex. The uridylyl-enzyme complex and Cys 160 loop are shown as ball-and-stick representations, where carbon, nitrogen, oxygen, phosphorus, and sulfur are depicted in black, blue, red, magenta, and yellow, respectively. Small spheres (light) represent ordered solvent molecules; a single large sphere indicates zinc. (b). Schematic diagram showing the superposition of UDP from the UMP/UDP enzyme complex upon UMP of the uridylyl-enzyme complex in the same color scheme as in (a). Non-hydrogen atom distances are indicated by dashed lines. Values shown indicate the average from both subunits. Parenthetical values are for the UMP/UDP enzyme. Residues identified in red boxes indicate interactions not present in the uridylyl-enzyme complex. Generated by use of MOLSCRIPT (Kraulis, 1991).

Cys 160 is positioned approximately 3.3 Å from O1 of the α-phosphoryl group (Figure 6b). Although this distance is slightly shorter than the normal range of thiol−oxygen hydrogen bond distances of 3.5 ± 0.1 Å (Ippolito et al., 1990), this interaction is not anticipated to be a major thermodynamic contributor to the coordination of the phosphate. In addition, a single ordered solvent molecule mediates an interaction between O2 of the phosphoryl group and the backbone amide of Asn 153 (of the Cys 160 loop) as well as the carbonyl O of His 166 (strand β8); Figure 6b depicts these interactions. A second ordered solvent is shared between O1 and O2, although this water is displaced most likely in the presence of the hexose-1-P. Collectively, the latter interactions provide evidence for at least two hydrogen bonds to the α-phosphoryl. Perhaps the most significant side-chain interaction to the phosphoryl group is that observed to Gln 168. The NH_2 moiety may form a bifurcated interaction with O2 and O5′ of the nucleotide (Figure 6).

Table 2: Gal-1-P Uridylyltransferase Active Site Consensus Sequence

organism[a]	amino acid										
E. coli	^{158}M	**G**	C	S	N	P	**H**	**P**	**H**	G	**Q**^{168}
H. influenzae	^{159}M	**G**	C	S	N	P	**H**	**P**	**H**	G	**Q**^{169}
H. sapiens	^{178}M	**G**	C	S	N	P	**H**	**P**	**H**	c	**Q**^{188}
M. musculus	^{159}M	**G**	C	S	N	P	**H**	**P**	**H**	c	**Q**^{169}
S. cerevisiae	^{174}M	**G**	C	S	N	l	**H**	**P**	**H**	G	**Q**^{184}
S. lividans	^{159}i	**G**	v	t	l	g	**H**	**P**	**H**	G	**Q**^{169}
S. typhimurium	^{156}M	**G**	C	S	N	P	**H**	**P**	**H**	G	**Q**^{166}
consensus	M	**G**	C	S	N	P	**H**	**P**	**H**	G	**Q**

[a] References: Lemaire & Mueller-Hill (1986) and Cornwell et al. (1987), *Escherichia coli*; Maskell et al. (1992), *Haemophilus influenzae*; Reichardt & Berg (1988) and Flach et al. (1990), *Homo sapiens*; Leslie et al. (1992), *Mus musculus*; Citron & Donelson (1984), *Saccharomyces cerevisiae*; Adams et al. (1988), *Streptomyces lividans*; Houng et al. (1990), *Salmonella typhimurium*.

This may allow the second amide hydrogen to participate in interactions to the β-phosphoryl group as it enters or exits the active site as UDP-hexose or hexose-1-P. Gln 168 is conserved strictly in all known sequences of the uridylyltransferase (Table 2). In the human enzyme, the mutation of Gln 168 to Arg (*E. coli* numbering system) renders the enzyme completely inactive (Fridovich-Keil & Jinks-Robertson, 1993). This latter mutation is the predominant cause of galactosemia among the Caucasian population (Reichardt et al., 1991; Leslie et al., 1992; Elsas et al., 1994).

Ribose Pucker. The change in the α-phosphorus position observed in the uridylyl intermediate relative to the UMP/UDP complex is due mostly to a rotation about the exocyclic C4′−C5′ bond. However, changes in the ribose ring pucker also play a role in the movement of the α-phosphorus toward the nucleophile, while maintaining the specific hydrogen bond interactions between the uracil base and NH 61, NH 78, and Oδ of Asp 78 (Figure 6b) as reported for the UMP/UDP enzyme complex (Wedekind et al., 1995). This conformational change in the ring pucker may be described in terms of the furanose phase angle, *P* (Altona & Sundralingham, 1972). The furanose phase angles for the riboses of the UMP/UDP enzyme complex are 164° and 183°, respectively. These values are typical of "S-conformation" nucleotides that exhibit a C2′−endo pucker (Saenger, 1984). In contrast, the *P* values for the uridylyl-enzyme complex are 128° and 121° (subunits I and II), which are consistent with a C1′-exo pucker. Figure 6b shows a superposition of the respective nucleotides, whereas Figure 6a emphasizes the influence this pucker change has made upon the environment of the ribose hydroxyl groups and the α-phosphoryl group. The ribose appears to act as a hinge that enables conformational adjustments to be made in the hexose diphosphate portion of the substrate, while keeping the uracil immobilized. Thus it is possible that the nucleotide binding mode observed for the inhibited UMP/UDP enzyme represents a normal though nonproductive substrate binding state prior to the first chemical displacement step. Since there is little energetic difference between C2′- endo and C1′-exo puckers, it appears that subtle alterations in the Cys 160 loop are essential for productive binding of the α-phosphoryl group whereas the uracil binding pocket is comparatively unchanged (Figure 6a).

Comparison to Other Phosphohistidines. Phosphorylated histidine residues have been observed previously in nucleoside diphosphate kinase (NDP) and succinyl-CoA synthetase

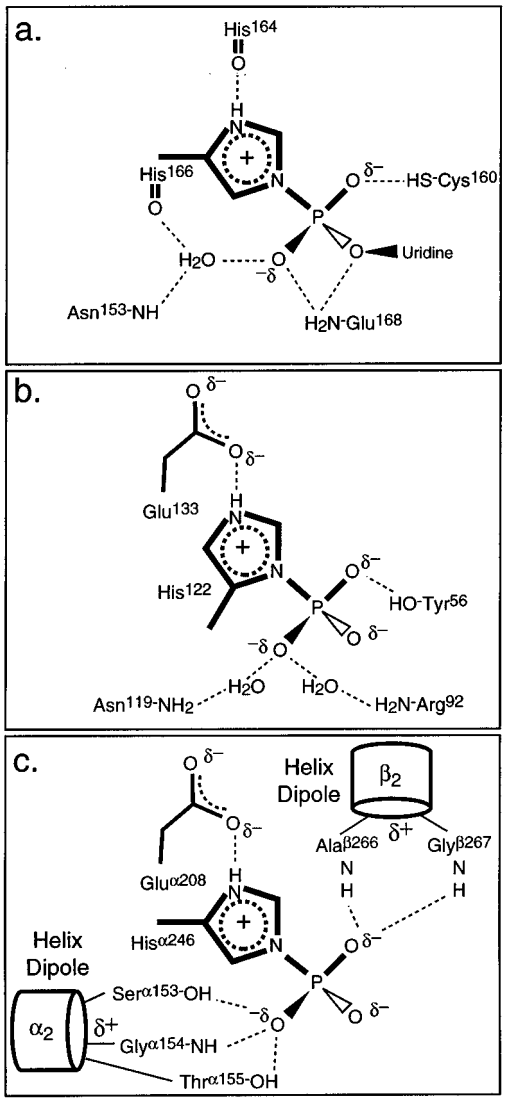

FIGURE 7: Schematic comparison of the uridylyl intermediate to other phosphohistidine enzymes. Dashed lines indicate potential hydrogen bond contacts. Residues were positioned for the sake of clarity rather than tertiary structure interpretation. Panels: (a) the uridylyl-enzyme; (b) NDP kinase from *Dictyostelium* (Moréra et al., 1995); (c) SCS from *E. coli* (Wolodko et al., 1994).

(SCS) (Wolodko et al., 1994; Moréra et al., 1995). In both cases these structures represent genuine reaction intermediates since the modified residue functions as an enzymatic nucleophile. Despite the absence of a nucleoside or analog thereof for these intermediates, it is useful to compare their structures to the uridylyl-enzyme in an effort to understand the structural attributes that contribute to phosphohistidine stability. Schematic drawings of the protein interactions to the phosphohistidines of these structures are shown in Figure 7. In the uridylyltransferase, the residues that coordinate the phosphoramidate are Cys 160 and Gln 168 (Figure 7a). Both NDP kinase and SCS utilize side chains as hydrogen bond donors to stabilize their intermediates as well. Hydroxyl groups from Tyr 56 of NDP kinase (Figure 7b) and Ser α153 and Thr α155 of SCS (Figure 7c) serve in this role. Both the uridylyltransferase and NDP kinase utilize water molecules to mediate interactions between the phosphoryl oxygens and the protein backbone in addition to direct backbone contacts (Figure 7a,b). Conformational changes

that may exclude the bound solvent have been invoked for the second half-reaction (Moréra et al., 1995) of NDP kinase in which a nucleoside diphosphate is phosphorylated. Therefore, in NDP kinase the interactions with water serve only to stabilize the intermediate. No such significant reorientation of the uridylylated histidine appears necessary for the uridylyltransferase. In contrast to the uridylyltransferase and NDP kinase, two of the phosphoryl oxygens of the SCS intermediate project toward the amino-terminal ends of two adjacent helices (Figure 7c). The favorable positive dipole of these α-helices, as well as direct hydrogen bonds to the amides from Gly α154, Ala β266, and Gly β267, has been proposed to contribute to the stability of the intermediate as well as the α−β dimer fold (Wolodko et al., 1994).

A significant difference between the phosphoryl-binding requirements for the uridylyl-enzyme on one hand and phosphoryl-enzymes on the other appears to be the use of more positive electrostatic binding of phosphoryl groups. Arg 92 interacts through a water molecule with the PO_3^{2-} of phospho-NDP kinase, and two positive helix dipoles interact with the PO_3^{2-} of phospho-SCS. The apparent greater electrostatic stabilization in the phosphoenzymes may be correlated with the fact that UDP-Glc is a higher energy uridylyl phosphotransfer agent ($\Delta G'^\circ = -10.3$ kcal mol^{-1} (Frey & Arabshahi, 1995)) than ATP is as a phosphotransfer agent ($\Delta G'^\circ = -7.8$ kcal mol^{-1}).[2] Less stabilization may be required to secure the UMP group from UDP-Glc than to stabilize the γ-phosphate from ATP on a histidine.[3] In contrast to the present structure, most kinases and ATPases include a metal ion and a lysine that serve to stabilize and orient the phosphoryl group that undergoes transfer (Herschlag & Jencks, 1990; Zheng et al., 1993; Smith & Rayment, 1996). For the uridylyltransferase, positional stability of reactive atoms is achieved though the presence of the phosphoryl monoester linkage to UMP, whereas a minimal electrostatic stabilization is provided by the side chains of Cys 160 and Gln 168.

The phosphohistidine of each structure described in Figure 7 appears to maintain a positively charged imidazole. In NDP kinase and SCS this observation is supported by the close proximity of the unphosphorylated imidazole nitrogen to the carboxylate oxygen of a nearby Glu (Figure 7b,c). In the uridylyltransferase Nδ2 is close to the carbonyl oxygen of His 164 (Figures 6b and 7a); the average C166−Nδ2−O164 angle is 125°. This falls within the range (119° ± 21°) tabulated by Ippolito et al. (1990) for imidazolium hydrogen bond donor/acceptor interactions in protein structures. The average Nδ2 166−O 164 distance is 2.5 Å with an estimated coordinate error of 0.15−0.175 Å (Figure 2). This interaction between Nδ2 166 and O 164 may be important in maintaining the orientation of the histidine in the active site.

The need to maintain a positively charged imidazolium group reflects the superior leaving group ability of the charged versus uncharged state. This is supported by model studies for the pH-dependent hydrolysis of UMPIm (Ruzicka & Frey, 1993). Rate constants from this study indicate that hydrolysis of zwitterionic UMPIm occurs 1500 times faster than for the corresponding monoanion. These studies reveal a large negative $\beta_{\text{leaving group}}$, indicative of a reaction rate dependent on leaving group (LG) stability with significant bond cleavage to the LG during the transition state (Ruzicka & Frey, 1993). The short hydrogen bond between Nδ2 166 and O 164 may serve as a means of temporarily eliminating charge on the modified imidazole and thus stabilize the intermediate uridylylhistidine until the initiation of the next partial reaction.

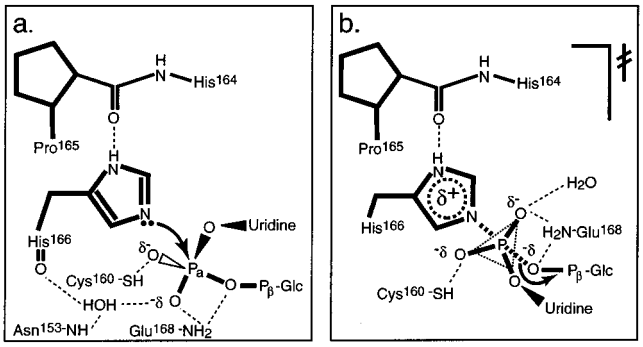

FIGURE 8: Schematic diagram of a single uridylyltransferase displacement reaction. Potential hydrogen bonds that may provide a significant means of stabilization are indicated as dashed lines. Panels (a) Attack of His 166 Nϵ2 on the substrate, UDP-Glc. (b) The trigonal-bipyramidal transition state indicating significant charge buildup on the His 166 imidazolium ring. The product of the displacement reaction is the present uridylyl-enzyme complex schematized in Figure 7a.

Perspectives on Catalysis. Figure 8 shows a schematic representation of the first displacement reaction. The uridylyl-enzyme complex represents the intermediate product of this reaction (Figure 7a). Upon binding the UDP-hexose substrate, His 166 attacks the α-phosphorus as shown in Figure 8a. On the basis of the present structure (Figure 6a) the hexose-1-P moiety must leave (and attack) opposite to Nϵ2, according to the known stereochemistry of each displacement reaction (eqs 2 and 3); the overall reaction proceeds with net retention of configuration about the α-phosphorus (Sheu et al., 1979; Arabshahi et al., 1986). Given this knowledge it may be speculated that the amide NH_2 group of Gln 168 interacts with the oxygens of both the α- and β-phosphoryl groups as depicted in Figure 8a. This seems reasonable given the position of this residue on sheet β8 (Figure 6a) and the importance of this residue as established by mutagenesis (Fridovich-Keil & Jinks-Robertson, 1993). Since the hexose-1-P leaving group has a pK_a of ∼7, there is no thermodynamic advantage in protonation of this position during the bond-breaking step of catalysis (Jencks, 1972). Instead, Gln 168 may serve to attenuate charge buildup at the β-phosphate position, which is consistent with its role as a simple hydrogen bond donor.

The role of Cys 160 is unclear even though it appears to interact with a nonbridging oxygen. A residue equivalent to Cys 160 exists in every uridylyltransferase sequence (Table 2) with the exception of that from *Streptomyces lividans*, which is reported to be a valine; however, this might be a sequence error.[4] If this is true, then conservation of this cysteine implies an important functional role for this amino acid residue. In general, cysteine is regarded as a weak hydrogen bond donor and very poor hydrogen bond acceptor (except when ionized). It is conceivable that the role of this

[2] The standard free energy of hydrolysis, $\Delta G'^\circ$, is determined at pH 7.0, 25 °C, and 1 mM free Mg^{2+}.

[3] ATP is also a high-energy AMP-group transferring molecule (ATP = AMP + PP_i; $\Delta G'^\circ = -10.9$ kcal mol^{-1}). The high energy of P_α−P_β cleavage in ATP is used to good effect in biological reactions (Frey & Arabshahi, 1995).

side chain is to prevent hydrolysis of the phosphohistidine by water by failing to provide a suitable hydrogen-bonding partner for an attacking water molecule. A hydroxyl side chain in the same position as Cys 160 would provide an avenue for the transfer of a proton from an attacking water molecule to the α-phosphate via hydrogen exchange. In contrast, a cysteine residue is able to provide a weak hydrogen bond to the α-phosphate group but would not be expected to participate in proton transfer.

The present structure implies that a single solvent molecule and the side chains of Gln 168 and Cys 160 are the only significant contributors to the electrostatic binding of the phosphoryl group. This observation is consistent with the standard free energy, $\Delta G'^{\circ}$, of the hydrolysis for the uridylyl−histidine bond and that for the conversion of UMPIm to UMP and imidazole, which are −14.7 and −15.4 kcal mol^{-1}, respectively (Arabshahi et al., 1996). Collectively, this implies that the formation of the enzyme intermediate at pH 7.0 is not associated with any significant increase in the stability of the phosphohistidine bond. Other conserved residues that were associated with the pyrophosphoryl oxygens of the previous UMP/UDP enzyme complex (Wedekind et al., 1995) appear to be unimportant in the overall reaction. Figure 6b emphasizes that Arg 31, Ser 161, and Asn 162 play no role in stabilizing the present uridylyl-enzyme complex, although these residues may participate in the initial binding of the substrate prior to its adoption of a productive conformation for catalysis.

It is interesting to question what is thermodynamically and kinetically necessary for this enzyme to function as a uridylyl transferase. The first requirement is a match between the free energy of hydrolysis of the phosphohistidine and the phosphoanhydride bond of UDP-Glc. At pH 7.0 $\Delta G'^{\circ}$ for the hydrolysis of the phosphoanhydride bond of UDP-Glc is −10.3 kcal mol^{-1}. This is more comparable to the $\Delta G'^{\circ}$ for the uridylyl-enzyme intermediate (−15.4 kcal mol^{-1}) than previously believed (Frey & Arabshahi, 1995; Arabshahi et al., 1996). Furthermore, under physiological conditions the thermodynamic difference between the uridylyl intermediate and the UDP-hexose is ameliorated by the greater concentration of substrates than enzyme. However, since the enzyme serves to equilibrate the thermodynamic distribution of UDP-hexoses with their corresponding hexose 1-phosphates in solution, its substantial rate constants for the transfer reactions are equally important to its function (Wong & Frey, 1974b). At higher pH, 8.5, the corresponding $\Delta G'^{\circ}$ values are −10.3, −9.9, and −12.6 kcal mol^{-1} for UDP-Glc, the enzyme intermediate, and UMPIm. The structural origin of the increased stability of the phosphohistidine bond at higher pH is not obvious, although it is certainly influenced by the protonation state of the His 166 imidazolium. Thus it appears that the structural role of the enzyme is to present the hexose phosphate to the phosphohistidine, while inhibiting the competing reaction with water or other substrates. In the absence of the structure of a complex with UDP-Glc or UDP-Gal it is difficult to predict exactly how this is accomplished.

[4] The sequence of the uridylyltransferase from *S. lividans* surrounding the valine is also different from that seen in all other species. An examination of the gene sequences from *Streptomyces*, including *galT*, shows an 80−90% preference for base G or C at codon positions 1 and 3. Consequently, sequencing compression errors in this region may have caused an incorrect reading frame to be assigned. Two nonconsecutive base deletions in the GC-rich region around Val 161 produce the protein sequence Met-Gly-Cys found in all other species.

CONCLUSIONS

The structure of the uridylyl-enzyme complex of galactose-1-phosphate uridylyltransferase has been determined. This reveals the covalent attachment of the UMP α-phosphorus to Nε2 of His 166 and represents a genuine reaction intermediate in the double-displacement mechanism. The specific interactions to the uracil and ribose moieties of the substrate appear to support those interactions reported previously (Wedekind et al., 1995). However, the α-phosphorus has moved 4 Å toward the nucleophile to engage in the formation of a phosphoramidate linkage. Rotations about the C4′−C5′ bond of UMP and the adoption of a C1′-exo pucker by ribose have facilitated intermediate formation. The side chains of Cys 160 and Gln 168 interact directly with the phosphoryl oxygens of the intermediate. Although the hexose-1-P substrate/product has not been located, it is likely that its β-phosphoryl oxygens interact with the side chain of Gln 168. The specific interactions of Gln 168 with the uridylyl intermediate suggest a possible source of enzyme dysfunction in the disease galactosemia. The stereochemistry of the reaction also suggests the importance of the NH_2 group of Asn 153 in recognition of the hexose-1-P β-phosphoryl group. Additional structural information for the uridylyltransferase will be necessary to locate the binding site of the hexose-1-P moiety.

ACKNOWLEDGMENT

We thank Dr. James B. Thoden for his technical assistance in collection of the X-ray data and Drs. George Reed and W. W. Cleland (University of Wisconsin) for helpful discussions. We thank the reviewer for suggesting that the sequence surrounding Val 161 in the uridylyltransferase from *S. lividans* might be incorrect. We also thank Siemens (Madison, WI) for the use of a Hi-STAR double detector system used for X-ray data collection.

REFERENCES

Adams, C. W., Fornwald, J. A., Schmidt, F. J., Rosenburg, M., & Brawner, M. E. (1988) *J. Bacteriol. 170*, 203−212.

Altona, C., & Sundralingham, M. (1972) *J. Am. Chem. Soc 94*, 8205−8212.

Arabshahi, A., Brody, R. S., Smallwood, A., Tsai, T.-C., & Frey, P. A. (1986) *Biochemistry 25*, 5583−5589.

Arabshahi, A., Ruzicka, F. J., Geeganage, S., & Frey, P. A. (1996) *Biochemistry 35*, 3426−3428.

Bernstein, F. C., Koetzle, T. F., Williams, G. J. B., Meyer, E. F., Jr., Brice, M. D., Rogers, J. R., Kennard, O., Shimanouchi, T., & Tasumi, M. (1977) *J. Mol. Biol. 112*, 535−542.

CCP4 (1994) *Acta Crystallogr. D50*, 760−763.

Citron, B. A., & Donelson, J. E. (1984) *J. Bacteriol. 158*, 269−278.

Cornwell, T. L., Adhya, S. L., Reznikoff, W. S., & Frey, P. A. (1987) *Nucleic Acids Res. 15*, 8116.

Elsas, L. J., Dembure, P. P., Langley, S., Paulk, E. M., Hjelm, L. N., & Fridovich-Keil, J. (1994) *Am. J. Hum. Genet. 54*, 1030−1036.

Field, T. L., Reznikoff, W. S., & Frey, P. A. (1989) *Biochemistry 28*, 2094−2099.

Flach, J. E., Reichardt, J. K. V., & Elsas, L. J. (1990) *Mol. Biol. Med. 7*, 365−369.

Frey, P. A., & Arabshahi, A. (1995) *Biochemistry 34*, 11307−11310.

Fridovich-Keil, J. J., & Jinks-Robertson, S. (1993) *Proc. Natl. Acad. Sci. U.S.A. 90*, 398−402.
Fukasawa, T., Segawa, T., & Nogi, Y. (1982) in *Methods in Enzymology* (Wood, W. A., Colowick, S. P., & Kaplan, N. O., Eds.) pp 584−592, Academic Press, New York.
Herschlag, D., & Jencks, W. P. (1990) *Biochemistry 29*, 5172−5179.
Houng, H.-S., Kopecko, D. J., & Baron, L. S. (1990) *J. Bacteriol. 172*, 4392−4398.
Ippolito, J. A., Alexander, R. S., & Christianson, D. W. (1990) *J. Mol. Biol. 215*, 457−471.
Jencks, W. P. (1972) *J. Am. Chem. Soc. 94*, 4731−4732.
Jones, T. A. (1985) in *Methods in Enzymology* (Wycoff, H. W., Hirs, C. H. W., & Timasheff, S. N., Eds.) pp 157−171, Academic Press Inc., New York.
Kabsch, W. (1976) *Acta Crystallogr. A32*, 922−923.
Kalckar, H. M. (1960) *Fed. Proc., Fed. Am. Soc. Exp. Biol. 19*, 984−990.
Kim, J., Ruzicka, F., & Frey, P. A. (1990) *Biochemistry 29*, 10590−10593.
Kraulis, P. J. (1991) *J. Appl. Crystallogr. 24*, 946−950.
Lecroisey, A., Lascu, I., Bominaar, A., Véron, M., & Delepierre, M. (1995) *Biochemistry 34*, 12445−12450.
Lemaire, H.-G., & Müller-Hill, B. (1986) *Nucleic Acids Res. 14*, 7705−7711.
Leslie, N. D., Immerman, E. B., Flach, J. E., Florez, M., Fridovich-Keil, J. L., & Elsas, L. J. (1992) *Genomics 14*, 474−480.
Levy, H. L., & Hammersen, G. (1978) *J. Pediatr. 92*, 871−877.
Luzzati, V. (1952) *Acta Crystallogr. 5*, 802−810.
Markus, H. B., Wu, J. W., Boches, F. S., Tedesco, T. A., Mellman, W. J., & Kallen, R. G. (1977) *J. Biol. Chem. 252*, 5363−5369.
Maskell, D. J., Szabo, M. J., Deadman, M. E., & Moxon, E. R. (1992) *Mol. Microbiol. 6*, 3051−3063.
Maxwell, E. S., Kurahashi, K., & Kalckar, H. M. (1962) in *Methods in Enzymology* (Colowick, S. P., & Chaplain, N. O., Eds.) pp 174−189, Academic Press, New York.
Moréra, S., Chiadmi, M., LeBras, G., Lascu, I., & Janin, J. (1995) *Biochemistry 34*, 11062−11070.
Pelton, J. G., Torchia, D. A., Meadow, N. D., & Roseman, S. (1992) *Biochemistry 31*, 5215−5224.
Phillips, J. N. J., Thomas, J. W. J., Annesley, T. M., & Quiocho, F. A. (1979) *J. Am. Chem. Soc 101*, 7120−7121.
Reichardt, J. K. V., & Berg, P. (1988) *Mol. Biol. Med. 5*, 107−122.
Reichardt, J. K. V., Packman, S., & Woo, S. L. C. (1991) *Am. J. Hum. Genet. 49*, 860−867.
Rodgers, D. W. (1994) *Structure 2*, 1135−1140.
Ruzicka, F. J., & Frey, P. A. (1993) *Bioorg. Chem. 21*, 238−248.
Ruzicka, F. J., Wedekind, J. E., Kim, K., Rayment, I., & Frey, P. A. (1995) *Biochemistry 34*, 5610−5617.
Saenger, W. (1984) *Principles of Nucleic Acid Structure* (Cantor, C. R., Ed.) pp 17−21, 55−61, Springer-Verlag, New York.
Segawa, T., & Fukasawa, T. (1979) *J. Biol. Chem. 254*, 10707−10709.
Seshadri, T. P., Viswamitra, M. A., & Kartha, G. (1980) *Acta Crystallogr. B36*, 925−927.
Sheu, K.-F. S., Richard, J. P., & Frey, P. A. (1979) *Biochemistry 18*, 5548−5556.
Smith, C. A., & Rayment, I. (1996) *Biophys. J. 70*, 1590−1602.
Teng, T. Y. (1990) *J. Appl. Crystallogr. 23*, 387−391.
Tronrud, D. E., Ten Eyck, L. F., & Matthews, B. W. (1987) *Acta Crystallogr. A43*, 489−501.
van Nuland, N. A. J., Boelens, R., Scheek, R. M., & Robillard, G. T. (1995) *J. Mol. Biol. 246*, 180−193.
Wedekind, J. E., Frey, P. A., & Rayment, I. (1994) *Acta Crystallogr. D50*, 329−331.
Wedekind, J. E., Frey, P. A., & Rayment, I. (1995) *Biochemistry 34*, 11049−11061.
Wolodko, W. T., Fraser, M. E., James, M. N. G., & Bridger, W. A. (1994) *J. Biol. Chem. 269*, 10883−10890.
Wong, L.-J., & Frey, P. A. (1974a) *J. Biol. Chem. 249*, 2322−2324.
Wong, L.-J., & Frey, P. A. (1974b) *Biochemistry 13*, 3889−3894.
Wong, L.-J., Sheu, K.-F. R., Lee, S.-L., & Frey, P. A. (1977) *Biochemistry 16*, 1010−1016.
Wu, J. W., Tedesco, T. A., Kallen, R. G., & Mellman, W. J. (1974) *J. Biol. Chem. 249*, 7038−7039.
Yang, S.-L. L., & Frey, P. A. (1979) *Biochemistry 18*, 2980−2984.
Zheng, J., Knighton, D. R., Ten Eyck, L. F., Karlsson, R., Xuong, N.-H., Taylor, S. S., & Sowadski, J. M. (1993) *Biochemistry 32*, 2154−2161.

BI9612677